Magnetization and ^{57}Fe and ^{119}Sn Mössbauer studies of magnetism in $RuR_{2-x}Ce_xSr_2Cu_2O_{10}$ (R=Eu, Gd)

I. Felner, E. Galstyan, R. H. Herber, and I. Nowik
Racah Institute of Physics, The Hebrew University, Jerusalem 91904, Israel
(Received 11 August 2003; revised manuscript received 14 April 2004; published 13 September 2004)

Magnetization and ^{57}Fe and ^{119}Sn Mössbauer effect studies of the magneto-superconducting $Ru_{1-x}Al_xEu_{1.5}Ce_{0.5}Sr_2Cu_2O_{10-\delta}$, $Ru_{0.99}{}^{57}Fe_{0.01}Gd_{1.5}Ce_{0.5}Sr_2Cu_2O_{10-\delta}$, and $Ru_{1-x}{}^{119}Sn_xGd_{1.5}Ce_{0.5}Sr_2Cu_2O_{10-\delta}$ systems, have been performed. The studies show that at $T_M \sim 160$ K, a sharp rise in magnetization occurs, not changing much down to $T_{M2} \sim 90$ K and displaying all along hysteresis loops. The coercive field increases when the temperature decreases, reaches a maximum at about 120 K and decreases again almost to zero around 90 K. At this temperature, a second, much larger rise in magnetization takes place, displaying typical ferromagnetic hysteresis loops. At $T_c \sim 30-35$ K the system becomes superconducting. The ^{57}Fe and ^{119}Sn Mössbauer spectra display at room temperature more than three inequivalent Fe or Sn sites, in accordance to their local environment. At low temperatures the spectra also display two to three magnetic inequivalent sites. Below T_M the spectra display magnetic hyperfine structure only for about 10% of the sample, the rest display magnetic order only below T_{M2}. While the magnetization studies tend to indicate that the material is homogeneous and around T_{M2} it undergoes some kind of spin or structural rearrangement; the ^{57}Fe and ^{119}Sn Mössbauer spectra tend to prove the occurrence of phase separation in these compounds. The two contradicting possibilities and an alternative approach are discussed in detail.

DOI: 10.1103/PhysRevB.70.094504 PACS number(s): 74.25.Ha, 74.10.+v, 75.25.+z, 76.80.+y

I. INTRODUCTION

The $RuR_{2-x}Ce_xSr_2Cu_2O_{10}$ (Ru-1222, R=Eu, Gd) materials display a magnetic transition at T_M=125–180 K and bulk superconductivity (SC) below T_C=32–50 K ($T_M \gg T_C$), depending on the R/Ce ratio and on the oxygen concentration.[1] The SC charge carriers originate from the CuO_2 planes and the magnetic order is confined to the Ru layers. The magnetic order does not vanish when SC sets in at T_C, but remains unchanged and coexists with the SC state. The exact nature of the magnetic structure of Ru-1222 is not yet known. The accumulated results are compatible with two alternative scenarios, both of which are used in understanding the qualitative features at low applied fields. (A) Going from high to low temperatures, the magnetic behavior is basically divided into two regions:[2] (i) At T_M the Ru sublattice becomes magnetically ordered, antiferromagnetically (AFM); (ii) at T_{M2} ($<T_M$), weak ferromagnetism (W-FM) sets in, which originates from canting of the Ru moments. This canting is a result of the tilting of the RuO_6 octahedra away from the crystallographic c axis.[3] At $T_C<T_{M2}$, SC is induced and both the SC and the W-FM states coexist intrinsically on a microscopic scale. (B) Detailed analysis of the magnetization under various thermal-magnetic conditions suggests a phase separation of Ru-1222 into FM and AFM [4–6] nanodomain species inside the crystal grains. A minor part of the material becomes FM at T_M, whereas the major part orders AFM and becomes SC at T_C. In this scenario, the unusual SC state is well understood.

To investigate the relationship between SC and magnetism in Ru-1222, we have attempted to replace Cu^{2+} by nonmagnetic Zn^{2+} ions.[7] Similar to all other Zn doped high T_C materials, tiny amounts of Zn are sufficient to suppress the SC state (T_C=38 K) and the material with 1.25 at.% of Zn is not SC down to 4.2 K. On the other hand, the magnetic state of the Ru sublattice is not significantly affected by the presence or absence of the SC state. This proves that the two states are practically decoupled. The wide ferromagnetic hysteresis loops which open at 5 K close themselves at T_{M2} =80 K, and reappear at $T_{M2}<T<T_M$. These observations tend toward preference of model (A) described above.

Here, we report the effect of nonmagnetic Sn^{4+} and Al^{3+} ions substitution for Ru^{5+}, on both SC and magnetic states of Ru-1222. It appears that the suppression rate of T_C is more moderate than in the Zn doped materials, and that about 7 at.% of Al ions are needed to destroy the SC state. Keeping in mind that such a substitution dilutes the magnetic RuO_2 layers, we show that Al substitution (up to 10%), shifts only T_{M2} to lower temperatures, but does not alter much T_M. On the other hand, the substitution of 5% of Sn affects dramatically both T_{M2} and T_M, and shifts them to lower temperatures.

Mössbauer studies (MS) of dilute ^{57}Fe or ^{119}Sn probes have proved to be a powerful tool in the determination of the magnetic nature of the probe's site location. When the Ru ions become magnetically ordered, they produce an exchange field on the Fe ions (or a transferred hyperfine field at the Sn nucleus) residing in this site. Both nuclei experience magnetic hyperfine fields leading to sextets in the observed MS spectra. Our present Mössbauer and magnetization studies tend to show that neither model (A nor B) described above is able to explain all observations. While the magnetization results are more easily explained by model A, the Mössbauer observations tend to support model B, they definitely show phase separation, at T_M only a *minor fraction* of the sample (10–20%) becomes magnetically ordered. At T_{M2}, also the *major fraction* becomes magnetically ordered.

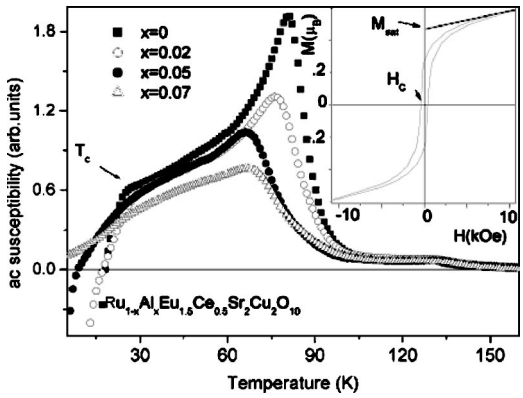

FIG. 1. The temperature dependence of the normalized real ac susceptibility of $Ru_{1-x}Al_xEu_{1.5}Ce_{0.5}Sr_2Cu_2O_{10}$. The inset shows the hysteresis loop at 5 K for $x=0.02$.

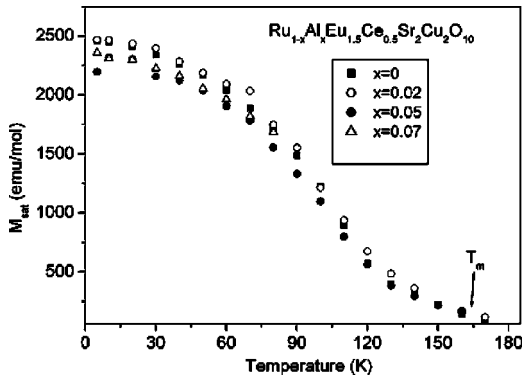

FIG. 2. The temperature dependence of the saturation moment M_{sat}, for $Ru_{1-x}Al_xEu_{1.5}Ce_{0.5}Sr_2Cu_2O_{10}$.

II. EXPERIMENTAL DETAILS

Samples were prepared by solid-state reactions as described elsewhere.[1–6] Each series of the materials reported was prepared at the same time under the same conditions. X-ray diffraction measurements confirmed the purity of the compounds, and indicate that within the instrumental accuracy, the doped samples have a tetragonal structure (space group I4/mmm) with the same lattice parameters as their parent compounds: $a=3.846(1), 3.844(1)$ Å and $c=28.72(1), 28.62(1)$ Å for $R=$Eu and Gd, respectively. DC magnetic measurements were performed in a commercial superconducting quantum interference device (SQUID) magnetometer. AC susceptibility was measured at ($H_{dc}=0$) by a homemade probe inserted in the SQUID, with an excitation frequency of 733 Hz and amplitude of 120 mOe. MS of ceramic samples containing ~1% ^{57}Fe and 2% ^{119}Sn (doped for Ru) were performed at various temperatures using a conventional constant acceleration drive and 50 mCi ^{57}Co:Rh and 5 mCi $Ba^{119m}SnO_3$ sources, respectively. The experimental spectra were analyzed in terms of several subspectra, by a least-squares fit procedure, corresponding to various models based on distributions of hyperfine interaction parameters. The ^{57}Fe and ^{119}Sn isomer shifts are relative to α-Fe and $BaSnO_3$ respectively, measured at room temperature.

III. EXPERIMENTAL RESULTS

A. The $Ru_{1-x}Al_xEu_{1.5}Ce_{0.5}Sr_2Cu_2O_{10}$ system

The temperature dependence of the normalized real ac susceptibility (χ') curves of samples with $x=0$, 0.02, 0.05, and 0.07 (all samples prepared simultaneously under the same conditions) are presented in Fig. 1. Doping of Al (and Sn) in Ru-1222 is reminiscent of the typical behavior of Al (and Sn) doped YBCO materials in which both ions substitute for Cu(1). Since the tetragonal Ru-1222 structure evolves from the YBCO one, we assume that both ions reside mainly in the Ru site. The negative susceptibility for samples with $x=0$, 0.02, and 0.05, indicate clearly that they are SC and that T_C is reduced from 36 K to 30 and 26 K, respectively. The $x=0.07$ and 0.1 samples are not SC and are magnetically ordered only. This is in contrast to the Zn (for Cu) doped samples in the Ru-1222 system, discussed above. Figure 1 shows that Al slightly affects the major peak position at T_{M2}. This peak [82(1) K for $x=0$] is shifted to 76, 70, 68 K for $x=0.02$, 0.05, and 0.07, respectively. Figure 1 also shows small peaks around 129(1) K, and close examination indicates that they are not affected by the presence of the Al ions.

Note that the peak position at T_{M2} *is not* T_M. The $\chi'(T)$ curves do not lend themselves to an easy determination of T_M, and for this purpose we measured the dc isothermal $M(H)$ curves at various temperatures. These curves are strongly dependent on the field (up to 2–4 kOe), until a common slope is reached (Fig. 1 inset). $M(H)$ can be described as: $M(H)=M_{sat}+\chi H$, where the saturation moment (M_{sat}) corresponds to the weak ferromagnetic (W-FM) contribution of the Ru sublattice, and χH is the linear paramagnetic contribution of R (Eu or Gd) and Cu. At low applied fields, *FM*-like hysteresis loops are opened, from which the remnant moments and the coercive fields (H_C) can be deduced.

Figure 2 shows the temperature dependence of M_{sat} obtained for all samples studied. The M_{sat} curves, become zero at $T_M(\mathrm{Ru})=162(2)$, (this is our definition for T_M) regardless of their Al concentration. Note that the M_{sat} values (at low temperatures) decrease with x.

The more interesting effects to be seen are exhibited in Fig. 3. The relatively wide FM hysteresis (Fig. 1, inset) loops which open at low temperatures ($H_C \sim 450-500$ Oe at 5 K) become narrow as the temperature increases and practically disappear around 60 K. However, above 80 K, small canted AFM-like hysteresis loops are reopened for all samples.[6,7] The $H_C(T)$ curves show a peak with a maximum at 120 K ($H_C \sim 150$ Oe) and become zero at T_M. Based on Figs. 1–3, we may conclude that the magnetic behavior of this system is as follows: (i) The SC materials and the non-SC one have basically the same T_M and a similar H_C trend. This means that the SC and magnetic states are decoupled from each other; (ii) the materials as a whole are W-FM at $T<T_{M2}$ and canted AFM ordered at $T_{M2}<T<T_M$; and (iii) the reappearance of hysteresis loops above T_{M2} is more consistent with model (A) described above. Below T_M, the AFM exchange

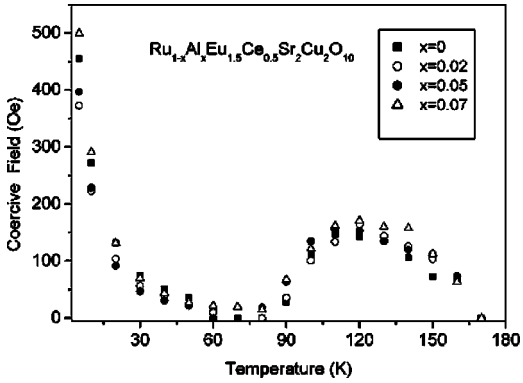

FIG. 3. The temperature dependence of the coercive fields for $Ru_{1-x}Al_xEu_{1.5}Ce_{0.5}Sr_2Cu_2O_{10}$.

energy increases with decreasing temperature and may overcome the coercive energies, which can lead to the observed unusual maximum and decrease of H_C.

B. $Ru_{1-x}Sn_xGd_{1.5}Ce_{0.5}Sr_2Cu_2O_{10}$ system

The $\chi'(T)$ plots of enriched Sn doped in Ru-1222 are presented in Fig. 4. It is readily observed that Sn substitution for Ru reduces T_C (39 K for $x=0$) to 26 ($x=0.02$) and 15 K ($x=0.05$), affects dramatically the peak position (91 K for $x=0$) and shifts it to 76 and 51 K for $x=0.02$ and $x=0.05$, respectively. In contrast to the Al doped materials (Fig. 1), the second minor peak in the $\chi'(T)$ curves is also affected by the presence of Sn, and shifted from 128 K (for $x=0$) to 122 and 115 K for $x=0.02$ and 0.05, respectively. This is consistent with the temperature variation of H_C (Fig. 5) which becomes zero at 80, 60, and 40 K and shows a maximum at 130, 130, and 100 K for $x=0$, 0.02, and 0.05, respectively. The hysteresis loops disappear at T_M which is 15 K lower for the $x=0.05$ sample. $M_{sat}(T)$ (not shown) which reaches zero at $T_M=170(2)$ for $x=0$ and 0.02, for $x=0.05$ is shifted to 155 K. The origin for the strong difference between the doped Sn and Al ion systems behavior, except for their different valence, leading to different oxygen content, cannot be fully explained at the present moment.

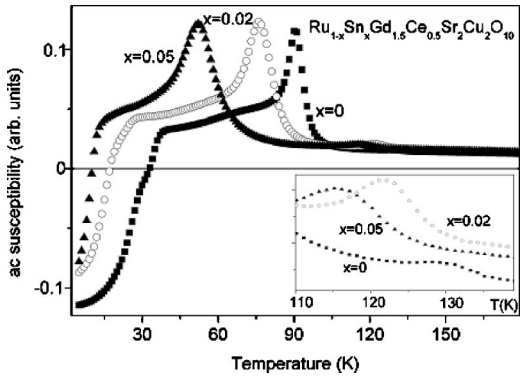

FIG. 4. The temperature dependence of the normalized real ac susceptibility curves of $Ru_{1-x}Sn_xGd_{1.5}Ce_{0.5}Sr_2Cu_2O_{10}$. The inset displays the second peak in an extended scale.

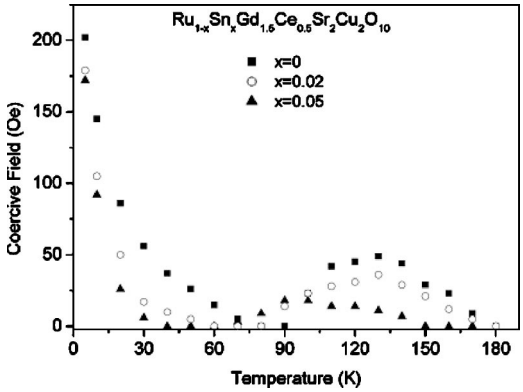

FIG. 5. The temperature dependence of the coercive fields for $Ru_{1-x}Sn_xGd_{1.5}Ce_{0.5}Sr_2Cu_2O_{10}$. Note the lower T_M for the $x=0.05$ sample.

The $\chi'(T)$ curve, not shown, for the 1% ^{57}Fe doped sample used for Mössbauer spectroscopy studies looks similar to that of the $x=0$ sample shown in Fig. 4. In that curve we observe: $T_C=21$ K, a major peak at 90 K, a minor peak at 123 K, and T_M at 170 K.

IV. MÖSSBAUER SPECTROSCOPY RESULTS

The samples $RuGd_{1.5}Ce_{0.5}Sr_2Cu_2O_{10}$ doped with ^{57}Fe (1%) and ^{119}Sn (2%) were studied by Mössbauer spectroscopy at temperatures 4.2 to 300 K. The experimental results indicate that while all Fe^{3+} ions enter the sample and are mainly located in the Ru site, only ~75% of the Sn^{4+} ions substitute Ru in the sample, the rest form probably the $SrSnO_3$ phase. Both the ^{57}Fe and ^{119}Sn Mössbauer spectra show magnetic hyperfine structure of a portion (minority fraction) of the probe ions at ~150–160 K. Due to the small size of this fraction, T_M cannot be determined precisely by MS. The fraction increases when lowering the temperature down to $T_{M2}\sim 90$ K and reaches values of 10–20%, the magnetic hyperfine fields reach almost saturation. At T_{M2} the rest of the probe ions (majority fraction) display magnetic hyperfine fields. At low temperatures all spectra exhibit very clearly the presence of at least two different subspectra. One subspectrum corresponding to the minority fraction, which ordered at T_M, and the other subspectra correspond to the majority fraction, which ordered at T_{M2}. We shall now describe in some detail the analysis of the experimental spectra observed, and discuss the possible interpretations of these observations.

A. ^{57}Fe:$RuGd_{1.5}Ce_{0.5}Sr_2Cu_2O_{10}$ Mössbauer spectra

Some of the experimental spectra are shown in Fig. 6 and the hyperfine interaction parameters obtained from the analysis of the spectra are given in Table I. The room temperature spectrum indicates that the ^{57}Fe probe ions are all trivalent. The ^{57}Fe ions replace Ru^{5+} ions, and thus have distorted environments, leading to a superposition of several subspectra corresponding to different local environments. The spectrum resembles to a great degree the spectrum observed for dilute iron in $YBa_2Cu_3O_7$.[8] The spectrum was least-squares

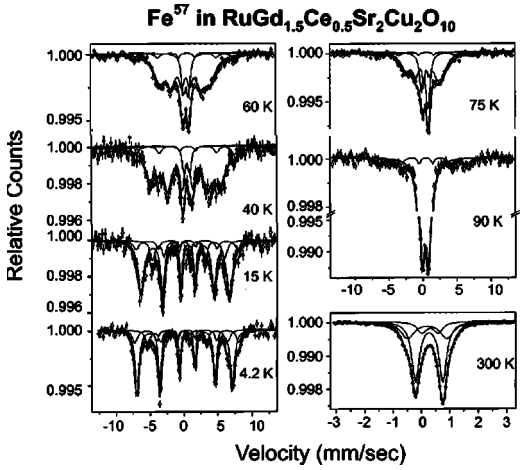

FIG. 6. Mössbauer spectra of 1% ^{57}Fe doped in $RuGd_{1.5}Ce_{0.5}Sr_2Cu_2O_{10}$, at various temperatures.

fitted with three subspectra, the parameters of which are given in Table II. It can be fitted, though less successfully, with a single asymmetric broad line quadrupole doublet, or a continuous asymmetric distribution of quadrupole doublets. The spectra below 150 to 90 K exhibit a superposition of two subspectra, the major one of which is the major high temperature paramagnetic quadrupole doublet while the minor one (~11%) is a magnetically split sextet. Below 90 K, an increasing part of the major doublet becomes magnetically split, with a distribution of hyperfine interaction parameters, according to the inequivalent iron probe locations. The spectra were analyzed in terms of three subspectra, one corresponding to the minority fraction ordered at T_M, the others to the majority fraction ordered at T_{M2}. The majority fraction displays two hyperfine fields, site I and site III in Table I, distinguishable only at the low temperatures 4.2 and 15 K. These two different hyperfine fields and very different quadrupole interactions result probably from iron probes in very different local environments, see Table II. In Fig. 7 the temperature dependences of the magnetic hyperfine fields and total magnetic fraction are shown, they are also given in Table I (where $\varepsilon = \frac{1}{4}e^2qQ$ for the paramagnetic cases, for the magnetically split spectra ε corresponds to its second order tensor projection along the magnetic field axis).

From the above observations we may conclude that, in the sample studied, if all iron probes respond equally to the Ru magnetic order,[9] there is a phase separation below $T_M \sim 160$ K. The present ^{57}Fe Mössbauer spectra are actually not that much different from those previously reported.[1,9] The differences are mainly due to the different composition and preparation procedures of the samples (in Refs. 1 and 9 the sample was $RuGd_{1.4}Ce_{0.6}Sr_2Cu_2O_{10}$).

B. ^{119}Sn:$RuGd_{1.5}Ce_{0.5}Sr_2Cu_2O_{10}$ Mössbauer spectra

Some of the experimental spectra are shown in Fig. 8 and the hyperfine interaction parameters obtained from the analysis of the spectra are given in Table III. The room temperature spectrum indicates that the ^{119}Sn probe ions are all tetravalent, replacing Ru^{5+} ions and have distorted environments, leading to a distribution of isomer shifts and quadrupole interactions. The spectrum was least-squares fitted with two subspectra, one (~75%) composed of a quadrupole doublet, corresponding to Sn in the Ru site of the compound and the other is composed of a single line with parameters similar to those of $SrSnO_3$ which may be present as an impurity phase. Indeed this single line subspectrum stays with the same relative intensity at all temperatures. The 75% subspectrum displays phase separation below 150 K. A minor part, ~10%, becomes magnetically ordered below 150 K, producing a transferred hyperfine field at the ^{119}Sn

TABLE I. The hyperfine interaction parameters derived from the analysis of the Mössbauer spectra of 1% ^{57}Fe in $RuGd_{1.5}Ce_{0.5}Sr_2Cu_2O_{10}$. P Int. stands for the paramagnetic fraction.

Temp	K	4.2	15	40	60	75	90	125
Int. 1	%	66(4)	70(4)	87(4)	82(3)	70(4)		
IS.	mm/s	0.36(1)	0.35(3)	0.36(4)	0.32(3)	0.39(3)		
ε	mm/s	−0.20(1)	−0.21(1)	−0.12(4)	−0.10(2)	−0.16(2)		
H_{eff}	kOe	433(1)	402(2)	309(4)	230(2)	166(3)		
Int. 2	%	17(4)	11(4)	9(3)	9(2)	11(3)	11(3)	11(3)
IS.	mm/s	0.47(4)	0.40(9)	0.32(9)	0.34(8)	0.44(12)	0.35(10)	0.40(10)
ε	mm/s	0.01(4)	−0.05(5)	−0.23(9)	−0.24(8)	−0.1(1)	−0.16(8)	−0.20(5)
H_{eff}	kOe	472(5)	461(9)	452(9)	462(9)	429(9)	393(8)	372(9)
Int. 3	%	19(4)	19(4)					
IS	mm/s	0.30(4)	0.35(4)					
ε	mm/s	0.28(6)	0.27(4)					
H_{eff}	kOe	362(4)	327(4)					
P. Int.	%			4(1)	9(4)	19(2)	89(3)	89(3)
IS.	mm/s			0.39(7)	0.44(7)	0.31(2)	0.35(3)	0.31(4)
ε	mm/s			0.42(5)	0.37(3)	0.47(3)	0.43(3)	0.40(4)

TABLE II. Hyperfine interaction parameters of the Mössbauer subspectra of 1% ^{57}Fe in $RuGd_{1.5}Ce_{0.5}Sr_2Cu_2O_{10}$, at room temperature. Sign of ε is not determined.

Site	Intensity %	Linewidth mm/s	Isomer shift mm/s	ε mm/s
1	57	0.32(2)	0.275(5)	0.480(5)
2	14(4)	0.40(5)	0.31(3)	0.29(3)
3	29(5)	0.58(5)	0.21(1)	0.69(2)
Average		0.41(5)	0.26(1)	0.51(3)

nucleus, while the major part becomes magnetically ordered only below ~80 K. In Fig. 9 the temperature dependences of the magnetic hyperfine fields of the two subspectra and the total magnetic fraction are shown. One notices that the ^{119}Sn Mössbauer spectra yield almost the same information as the ^{57}Fe Mössbauer spectra, only with less accuracy due to the inherently broader lines, smaller hyperfine fields (transferred hyperfine fields), and the presence of the $SrSnO_3$ impurity.

V. DISCUSSION

Without a detailed magnetic structure from neutron diffraction studies, it is difficult to determine the exact nature of the magnetic structure in the Ru-1222 system. However to account for the magnetic properties of the Ru sublattice we consider the following facts. Figures 2 and 3 show that for the Al doped Ru-1222 materials the SC and the non-SC materials have basically the same T_M, H_C, and M_{sat}. This means that the SC state (which is confined to the Cu-O layers) and magnetic state of the Ru sublattice are practically decoupled from each other. On the other hand, for the material with 5 at.% of Sn^{4+} ions, a significant shift is observed in the major peak position (about 40 K) and both the minor peak in the ac susceptibility curve and T_M are lowered by 15 K from the parent compound. We suggest a general picture in which all doped and undoped materials have basically a similar magnetic structure, which is not affected by the presence of nonmagnetic ions in the Ru site. Our magnetic measurements exhibited in Figs. 1–5, are compatible with our qualitative model (A). In this scenario, *all* the Ru ions behave in the same manner as follows: (i) The small peak observed in Figs. 1 and 4 indicates that at low applied fields the Ru sublattice becomes AFM ordered at T_M (160–170 K). At high magnetic field, the Ru moments are realigned through a spin-flip process, to form the AFM-like shape hysteresis loops observed below T_M;[7,10] (ii) at T_{M2} (80–100 K), a W-FM ordering is induced, which originates from canting of the Ru moments, which arises from the fact that the RuO_6 octahedra tilt away from the crystallographic c axis.[3] The FM-like hysteresis loops obtained at low temperatures are also consistent with W-FM order in this system. To emphasize this point, in range (i) the AFM hysteresis loops are induced by the applied fields whereas, in range (ii) the FM like hysteresis loops are caused by the crystallographic effect; and (iii) at T_C=20–40 K, SC which is confined to the CuO_2 layers, is induced. Below T_C, both SC and W-FM states coexist and

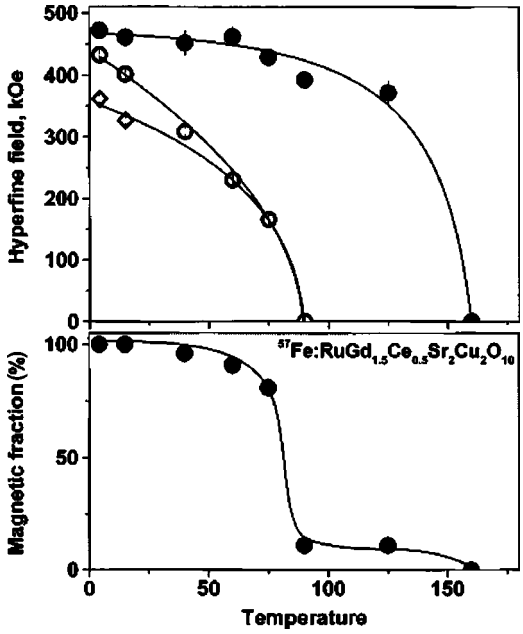

FIG. 7. Temperature dependence of the hyperfine fields and total magnetic fraction for 1% ^{57}Fe doped in $RuGd_{1.5}Ce_{0.5}Sr_2Cu_2O_{10}$.

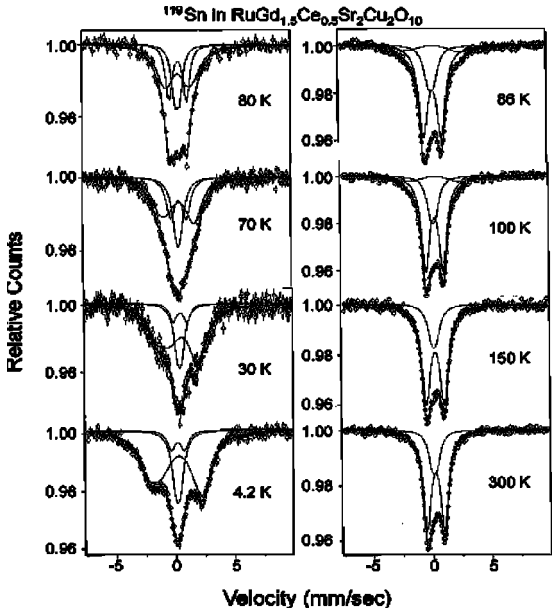

FIG. 8. Mossbauer spectra of 2% ^{119}Sn doped in $RuGd_{1.5}Ce_{0.5}Sr_2Cu_2O_{10}$ at various temperatures.

TABLE III. The hyperfine interaction parameters derived from the analysis of the Mössbauer spectra of 2% ^{119}Sn in $RuGd_{1.5}Ce_{0.5}Sr_2Cu_2O_{10}$. The IS of site 3 is that of site 1.

Temp K	Int. 1 % ±3	IS. mm/s ±0.03	ε mm/s ±0.04	Int. 2 % ±3	IS. mm/s ±0.02	Int. 3 % ±3	ε mm/s ±0.04	H_{eff} kOe ±4
4.2	9	0.26	0.56	21	0.26	70	−0.17	35
30	12	0.31	0.6	21	0.25	67	−0.27	27
50	6	0.31	0.65	25	0.32	73	−0.16	24
70	31	0.31	0.7	30	0.27	39	−0.14	24
80	40	0.31	0.74	24	0.26	36	−0.07	22
86	68	0.3	0.75	23	0.19	9	−0.05	36
100	70	0.26	0.74	23	0.17	7	−0.04	34
120	74	0.26	0.75	22	0.17	4	−0.07	34
150	78	0.26	0.75	22	0.17	0		
200	77	0.24	0.71	23	0.13			
300	77	0.21	0.73	23	0.11			

the two states are practically decoupled. Model A is also supported by electron spin resonance (ESR) studies.[11] The phase separation model (B) described above,[4–6] cannot be reconciled with the reopening of hysteresis loops above T_{M2}, and as a result does not account for the peak observed in H_C (Figs. 3 and 5) in both systems studied. According to this scenario, the hysteresis loops opened at T_M would remain all the way down to low temperatures and H_C would increase continuously, or at least remain constant.

On the other hand, our detailed MS analysis presented here (Figs. 6–9) indicates with little doubt the occurrence of a second magnetic phase at $T > T_{M2}$, inconsistent with model A. This is also supported by muon spin rotation studies.[12] A possible reason for this second phase is the inhomogeneity of the oxygen content across the sample. We offer therefore a *third* scenario (C), which is based on the two (A) and (B) models, and is consistent with our present observations. We propose that at $T_M \sim 160$ K, a nanoparticle minority fraction (10–20%) of the material starts to order magnetically as a slightly canted AFM, displaying hysteresis loops. When the temperature is lowered, the AFM alignment of the spins strengthens, and H_C goes through a maximum around 120 K, and then decreases toward lower temperatures. The majority fraction becomes W-FM ordered at T_{M2} and displays the typical FM-like hysteresis loops. At $T_C \sim 30$ K the whole system becomes superconducting. This picture is consistent with our magnetization and MS studies, as well as with the recent (μSR) studies.[12] All the previous magnetization studies[4–6] and ESR studies[11] can also be accommodated within this approach. Since the oxygen content of the sample affects the phase separation and magnetic structure and also the distribution of the iron probe environments, it is not surprising to find a rough correlation between the three MS sites in the magnetically ordered temperature region to those three sites found in the paramagnetic region, Tables I and II.

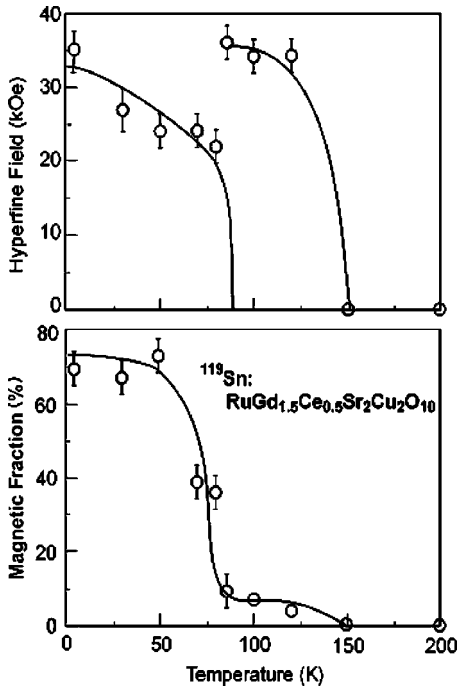

FIG. 9. Temperature dependence of the hyperfine fields, and total magnetic fraction (reaching only 75% due to the nonmagnetic impurity present in the sample).

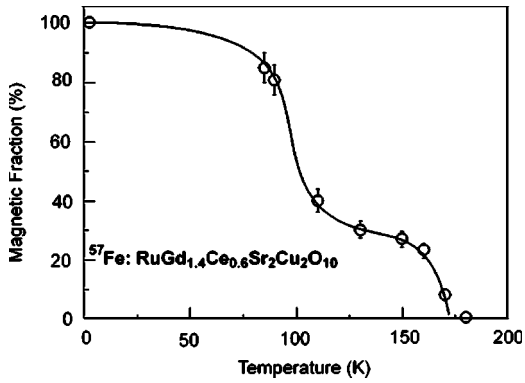

FIG. 10. Temperature dependence of the magnetic fraction in the Mössbauer spectra reported in Refs. 1 and 9.

Another noteworthy point is that the ^{57}Fe MS data here presented, differ only slightly from those published in our previous publications.[1,9] It is well accepted that the SC and magnetic properties of the Ru-1222 system depend strongly on the R/Ce ratio and on the oxygen concentration. The later is very sensitive to the preparation conditions and differs from sample to sample. The ratio Gd/Ce here is 3, whereas in Refs. 1 and 9 it was 2.33. Moreover, the slightly different preparation conditions as well as the Fe concentration, all may lead to a change in oxygen distribution in the local environment around the Fe ions as probes. As a result, the minor fraction concentration as detected by the Fe probe was different in Refs. 1 and 9, ~30%, Fig. 10, led to an interpretation of the spectra, different than that presented here. In fact an analysis of the old spectra[1,9] with the assumptions made for the analysis of the present spectra (presence of two to three subspectra) led to much better least-squares fit results than those presented originally.[1,9]

ACKNOWLEDGMENTS

This research was supported by the Israel Science Foundation (2004), and by the Klachky Foundation for Superconductivity.

[1] I. Felner, U. Asaf, Y. Levi, and O. Millo, Phys. Rev. B **55**, R3374 (1997).
[2] I. Felner, U. Asaf, and E. Galstyan, Phys. Rev. B **66**, 024503 (2002).
[3] C. S. Knee, B. R. Rainford, and M. T. Weller, J. Mater. Chem. **10**, 2445 (2000).
[4] Y. Y. Xue, D. H. Cao, B. Lorenz, and C. W. Chu, Phys. Rev. B **65**, 020511(R) (2001).
[5] Y. Y. Xue, B. Lorenz, A. Baikalov, D. H. Cao, Z. G. Li, and C. W. Chu, Phys. Rev. B **66**, 014503 (2002).
[6] Y. Y. Xue, B. Lorenz, D. H. Cao, and C. W. Chu, Phys. Rev. B **67**, 184507 (2003).
[7] I. Felner, E. Galstyan, V. P. S. Awana, and E. Takayama-Muromachi, Physica C (to be published).
[8] E. R. Bauminger, M. Kowitt, I. Felner, and I. Nowik, Solid State Commun. **65**, 123 (1988); D. Hechel, I. Nowik, E. R. Bauminger, and I. Felner, Phys. Rev. B **42**, 2166 (1990).
[9] I. Nowik, I. Felner, and U. Asaf, Hyperfine Interact. **141**, 213 (2002).
[10] V. P. S. Awana and E. Takayama-Muromachii, Physica C **390**, 101 (2003).
[11] K. Yoshida, H. Kojima, and H. Shimizu, J. Phys. Soc. Jpn. **72**, 3254 (2003).
[12] A. Shengelaya, R. Khasanov, D. G. Eshchenko, I. Felner, U. Asaf, I. M. Savic, H. Keller, and K. H. Muller, Phys. Rev. B **69**, 024517 (2004).